Non-Wilms' Renal Tumors

39

Archana Puri, Kiran Mishra, and Rama Anand

39.1 Congenital Mesoblastic Nephroma

39.1.1 Incidence and Epidemiology

CMN or "Bolande's tumor" despite its rarity is still one of the most common congenital tumors [1]. The term CMN was coined by Bolande in 1967 to emphasize its congenital nature and predominant mesenchymal component in its histology [1]. It is the most common solid renal tumor of neonates and infants younger than 6 months. Although it accounts for less than 5% of all pediatric renal tumors, 67% of all renal tumors in infants younger than 6 months are CMN [2]. Its estimated incidence is 1:500,000 infants [3]. The median age at diagnosis for CMN in most series is 2 months, with up to 80% of all cases reported in the first month of life and up to 90% in infants younger than 1 year with only few sporadic reports in older children and adults. It shows sex predilection with a male/female ratio of 1.5:1 [1, 2].

A. Puri (✉)
Department of Pediatric Surgery, Vardhman Mahavir Medical College and Safdarjung Hospital, New Delhi, India

K. Mishra
Department of Pathology, University College of Medical Sciences, New Delhi, India

R. Anand
Department of Radiodiagnosis, Lady Hardinge Medical College, New Delhi, Delhi, India

39.1.2 Clinical Presentation

It often presents as an incidentally diagnosed asymptomatic abdominal mass, noted either since birth or soon after birth. This abdominal mass may even get detected prenatally usually in association with maternal polyhydramnios; CMN is the most common renal tumor that is diagnosed on antenatal ultrasonography (USG). Perinatal presentations are often associated with premature labor; rarely however they may present with hydrops fetalis, congestive heart failure (due to hypertension, or arteriovenous shunting), or tumor rupture causing hemoperitoneum and shock. Rare postnatal presentations may include metabolic disturbances with hypercalcemia, nephrocalcinosis, and syndrome of increased renin secretion. Although hypercalcemia can occur in 1–2% of renal tumors of childhood, it is most commonly reported with malignant rhabdoid tumor of the kidney (MRTK) and rarely in CMN [4]. It is a paraneoplastic phenomenon due to ectopic production of parathormone and prostaglandin E2, manifesting with nonspecific symptoms such as anorexia, vomiting, floppiness, and constipation. However, severe hypercalcemia (>15 mg%) can present with severe abdominal pain, persistent vomiting, extreme weakness, severe dehydration, rapid deterioration of renal function, coma, and death [4]. Serum calcium levels in such conditions can act as a biochemical tumor marker, with normalization of calcium levels after complete tumor resection.

Y. K. Sarin (ed.), *Wilms' Tumor*, https://doi.org/10.1007/978-981-19-3428-5_39

Increased renin secretion can either occur from the tumor or be because of local ischemia produced by compression of normal glomeruli by tumor, and it often manifests as hypertension [5].

39.1.3 Radiological Diagnosis

Pathognomonic ultrasonographic (USG) features of CMN are of a small round tumor with indistinct margins and characteristic hypoechoic rim around the tumor. Further diagnostic clarity is provided by contrast enhanced computerized tomography (CECT), which often shows solid-cystic tumor with indistinct demarcation from the normal kidney with **double-rim sign** (tumor appears having two boundaries). The double-rim sign correlates with hypoechoic ring on Doppler USG [2]. It is hypothesized and often confirmed on histological examination that hypoechoic ring is caused by slow blood flow in dilated blood vessels and entrapped nephrons at the tumor periphery. Another characteristic radiological finding of CMN is the presence of **intra-tumor pelvis**, signifying that part of the pelvis is encapsulated by the tumor [2]. Although it may be difficult to differentiate CMN from WT radiologically, it is worthwhile to note that CMN tends to infiltrate the kidney, encapsulating the pelvis rather than forming a pseudocapsule as noted in WT (Fig. 39.1).

39.1.4 Pathology

At gross examination, CMN appears to be an infiltrative mass with ill-defined margins and no capsule. On cut section, it is predominately solid with whorled, firm, yellow surface with rubbery consistency (Fig. 39.2). Histologically, they have uniform spindle-shaped cells arranged in bundles with trapping of normal tubules and glomeruli at the periphery of the tumor. Early age of onset and infiltrative growth pattern of CMN with entrapment of tubules and glomeruli rather than the formation of tubular structures help to differentiate

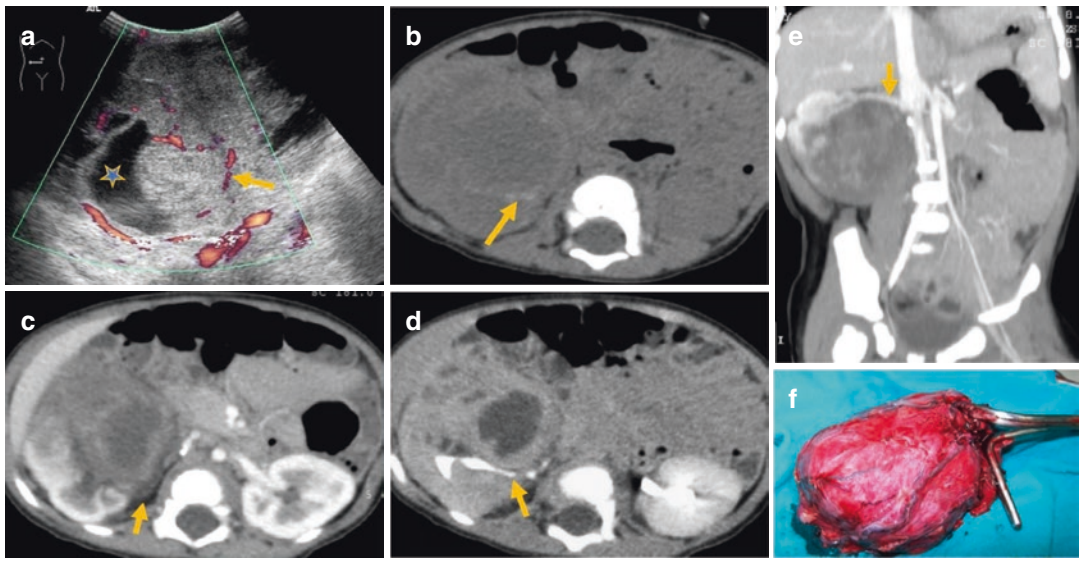

Fig. 39.1 Nine-month-old boy with right lumbar mass noted since 1 month. (**a**) Axial color Doppler image shows a large, heterogeneous mass with anechoic areas due to necrosis (*); solid area shows some peripheral and internal vascularity (arrow); (**b**) Non-contrast CT scan shows a hypodense mass with areas of hemorrhage (arrow); (**c**) CECT shows mildly enhancing mass arising from medial aspect of the lower pole of the right kidney showing non-enhancing necrotic areas, indistinct demarcation from the normal kidney, double-rim sign, and involvement of the renal sinus; (**d**) delayed phase image shows calyceal distortion by the mass and intra-tumor pelvis (arrow); (**e**) coronal section shows the mass displacing the inferior vena cava (IVC) and right renal artery (arrow) without evidence of invasion or encasement; (**f**) photograph of resected tumor—histopathology revealed cellular variant of CMN

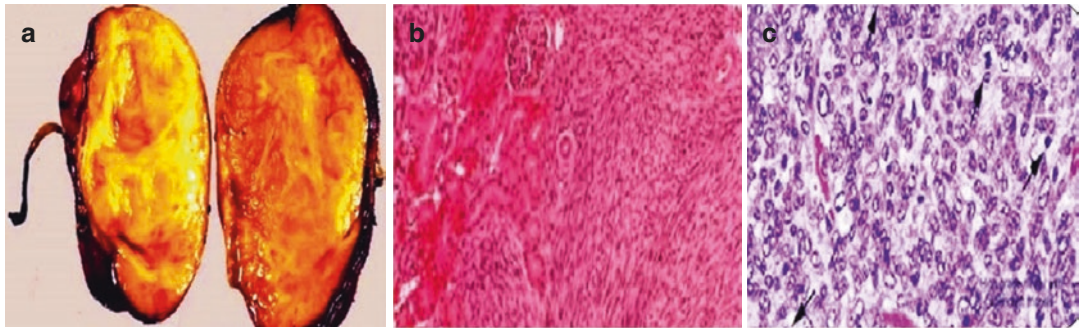

Fig. 39.2 (**a**) Gross specimen showing large unencapsulated large renal tumor with firm yellowish-white whorled cut surface suggestive of CMN. (**b**) Classic CMN showing intersecting bundles of spindle cell pushing through into the kidney substance with low grade nuclei with very few mitoses. (**c**) Cellular CMN with polygonal and spindle cells with high mitotic rate (black arrow)

it from WT. Fine needle aspiration cytology (FNAC) in CMN, unlike WT, is usually hypocellular and is composed of cohesive clusters of spindle cells with round to oval nuclei with fine chromatin and indistinct nucleoli [6]. Blastemal component is conspicuously absent. Thus, on FNAC, WT treated with preoperative chemotherapy or WT with stromal predominance forms close differentials for CMN.

There are three histological subtypes or variants of CMN based on cellularity and mitosis, namely, classical (24%), atypical or cellular (66%), and mixed (10%) (Fig. 39.2). Atypical or cellular variant is also called as malignant mesenchymal nephroma of the kidney and is characterized by aneuploidy and high mitotic index (8–30 mitoses per 10 high power fields) and exhibits cystic degeneration, intra-tumoral hemorrhage, and necrosis [1, 2, 7]. Classical variant morphologically resembles infantile fibromatosis of the renal sinus, and cellular variant is identical to infantile fibrosarcoma. Cytogenetic and molecular studies have documented chromosomal changes especially trisomy 11 and translocation **t(12:15) (p13; q25) with ETV6 NTRKS gene fusion** in most cases of cellular CMN, as is also noted in infantile fibrosarcoma [1, 8]. While CMN exhibits strong immunoreactivity for vimentin, fibronectin, and actin, it shows only focal or weak desmin positivity [1]. It is worthwhile to mention that cellular variant has a delayed age at presentation (121 ± 236 days versus 6.6 ± 7.4 days for classical variant). Imaging findings may also assist to predict the likely pathological variant. Presence of foci of hemorrhage and degenerative cystic, necrotic changes in the tumor on imaging are more consistent with the cellular histology, while classical variety is characterized by the presence of hypoechoic rim and a large solid component in the tumor. Presence of extrarenal extension of tumor in adjacent surroundings is also consistent with cellular histology [7].

39.1.5 Management

Although previously, all primary renal tumors diagnosed prior to 6 months of age were considered benign CMN and were treated with upfront radical nephroureterectomy (RN) alone ensuring no spillage, tumor-free margins, and lymph node sampling, a lot of rethinking had occurred recently for infants more than 3 months of age [9]. It was observed that likelihood of renal tumor being benign decreases drastically after 3 months and there may be a need to consider cellular or mixed variant of CMN or even an alternate diagnosis of WT in them [7]. The infiltrative nature of CMN with its tendency to extend into hilar and perirenal soft tissue excludes partial nephrectomy as a surgical option for these infants [10]. Unlike WT, adjuvant postoperative ChT may be required in few situations in CMN such as incomplete exci-

sion and positive tumor margins (PTMs) and with cellular or mixed histology, particularly in those who are more than 3 months of age [1, 2].

Overall recurrence rate for CMN is 5%, but with cellular histology, it rises to 10–20%. Cellular variant of CMN is associated with even distant metastasis to the lungs and brain and an unacceptably high mortality of 57% in this group of patients [10]. Recurrence usually occurs within 1 year after surgical resection. Recurrence rate increases with invasion of renal sinus and vascular invasion and in stage III tumors. Surgery remains the mainstay of treatment even for recurrent or metastatic disease. Adjuvant ChT with vincristine (VCR) alone or in combination with actinomycin-D (AMD) and cyclophosphamide (CTX) is the usual first-line ChT for recurrent or metastatic disease [10]. It is postulated ETV6 NTRKS gene fusion not only renders them chemosensitive but also provides a possibility of targeted therapy in children with cellular CMN with recurrent or metastatic disease. Targeted therapy with larotrectinib, crizotinib, and entrectinib is under trial and may hold promise in refractory cases of cellular CMN [10].

Overall prognosis of CMN is favorable, but stringent follow-up is mandatory for a minimum of 18 months after surgical excision in all patients with CMN [10]. Event-free survival (EFS) and overall survival (OS) of even cellular CMN is 85% and 90%, respectively.

39.2 Malignant Rhabdoid Tumor of the Kidney

39.2.1 Incidence and Epidemiology

MRTK is a rare but highly aggressive renal neoplasm and accounts for 2% of pediatric renal tumors [11]. Originally, it was thought to represent the monophasic sarcomatoid variant of WT [11]. However, later in 1981, it was identified as a separate entity probably arising from primitive cells involved in the formation of renal medulla [12, 13]. Its frequent association with primary and metastatic central nervous system (CNS) tumors subsequently leads to speculations of its probable neuroectodermal origin [12]. Moreover, it can occur in extrarenal locations including the liver, soft tissues, lung, skin, heart, and brain, suggesting its origin from a non-organ-specific mesenchymal cell. It derives its name from its histological appearance, which resembles rhabdomyosarcoma (RMS), but undoubtedly it is not of myogenic origin and does not show any skeletal muscle markers on immunohistochemistry (IHC). The median age at presentation for MRTK is 11 months (range: 0 to 4.5 years), and it is extremely rare beyond 5 years of age [14, 15]. Age at diagnosis is a significant prognostic factor for survival in children with MRTK; infants have a dismal prognosis as compared to older children.

39.2.2 Clinical Presentation

It often presents as a unilateral abdominal mass with almost equal probability to occur on either side and is bilateral in 4% of patients [13]. Although a definitive diagnosis of MRTK is often made on histopathology, **presence of large renal tumor in a young infant, especially when associated with hematuria, hypercalcemia, and diffuse hematogeneous and lymphatic spread, suggests a diagnosis of MRTK** [13]. Hematuria (both gross and microscopic) is seen more frequently with MRTK as compared to a WT due to its more central origin from the renal medulla leading to early invasion of the renal pelvis. Gross and microscopic hematuria was reported more frequently (59% and 76%, respectively) in children with MRTK as compared to children with WT (18% and 24%, respectively) [13]. Similarly, fever was noted in 45% of children with MRTK as compared with 22% with WT. While 71% of patients with MRTK had more advanced stage at presentation (stage III: 44%; stage IV: 27%), 67% of children with WT had stage I (41%) and stage II (26%) disease [13]. Presence of hypercalcemia (with serum calcium of more than 10.5 mg%) is quite characteristic of MRTK and is seen in nearly one-fourth of cases [13]. The association of MRTK with synchronous and metachronous primary and secondary intracranial malignancy

is well-documented. The primary brain tumors tend to occur in midline commonly in the posterior fossa and include medulloblastoma, ependymoma, primitive neuroectodermal tumors, and cerebellar and brainstem astrocytoma [11]. They may also extend into the inferior vena cava and renal vein.

39.2.3 Radiological Diagnosis

Although imaging findings of MRTK are indistinguishable from WT, there are some telltale signs that may provide subtle hints to diagnose RTK (Fig. 39.3). USG usually shows a large lobulated mass with heterogeneous echogenicity, which may have intravascular extension into the renal vein or inferior vena cava (IVC). **Presence of a large (5–12 cm), lobular, central, intrarenal mass, with ill-defined margins (57%) in a young child, extending beyond the renal medulla into the renal sinus and renal pelvis, is quite characteristic of MRTK** [11, 14]. Another classical radiological sign of MRTK is perilobular calcification that is noted in 45% of cases as compared to egg shell calcification seen in less than 10% of children with WT. [12, 14] Agrons et al. found peripheral crescent of fluid attenuation, representing subcapsular hematoma or tumor necrosis, in 71% of children with MRTK. However, this is not pathognomonic of MRTK as it is seen in 12% of other more common pediatric renal neoplasms [11].

39.2.4 Pathology

Grossly, the tumors are unencapsulated and often have extensive areas of hemorrhage and necrosis. Both primary and metastatic MRTK comprise of sheets of monomorphic tumor cells with abundant eosinophilic cytoplasm and large eccentric nuclei with prominent **owl eye** nucleoli and have pathognomonic **intracytoplasmic pink inclusions adjacent to areas surrounding necrosis** (Fig. 39.4). On ultrastructural examination, it shows similarity to RMS with plenty of eosinophilic cytoplasm containing filamentous inclusions, which shows positive immunoreactivity to vimentin and focal cytokeratin, but not of actin or myosin as seen in tumors of myogenic origin [12]. Although no IHC staining is considered pathognomonic of MRTK, genetic abnormalities leading to inactivation of the **Hsnf5/INI-1tumor suppressor gene on chromosome 22** is considered quite characteristic of both renal and extrarenal rhabdoid tumors [8]. It is noteworthy that for all other renal tumors except MRTK, IHC staining for integrase interactor 1 **(INI-1)** shows nuclear positivity [8].

39.2.5 Management

RN and LN sampling were combined with alternating cycles of carboplatin and etoposide with cyclophosphamide for 24 weeks and radiotherapy (XRT) for all stages of MRTK earlier [16].

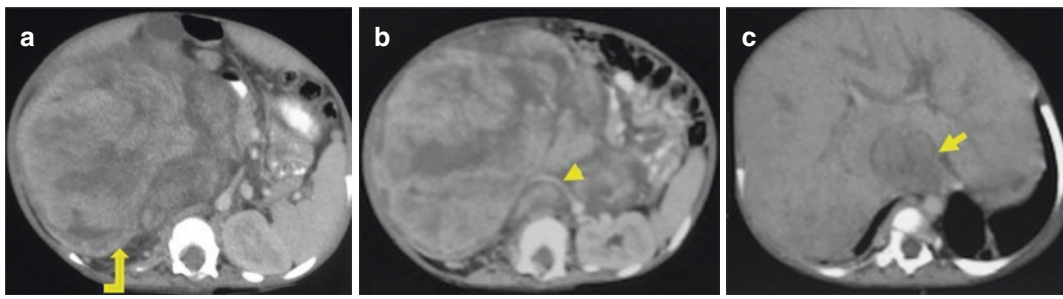

Fig. 39.3 Fifteen-month-old female child presented with right-sided renal mass and hematuria since 1 year of age. CECT scan axial images (**a**, **b**) show a large lobulated solid well-circumscribed mass replacing the right kidney. Mass shows marked necrosis and is involving the renal hilum, with extension into the right renal vein and IVC. The right renal artery is displaced anteriorly (arrowhead) by the dilated IVC filled with tumor thrombus. (**c**) Large suprahepatic IVC thrombus (arrow) is seen

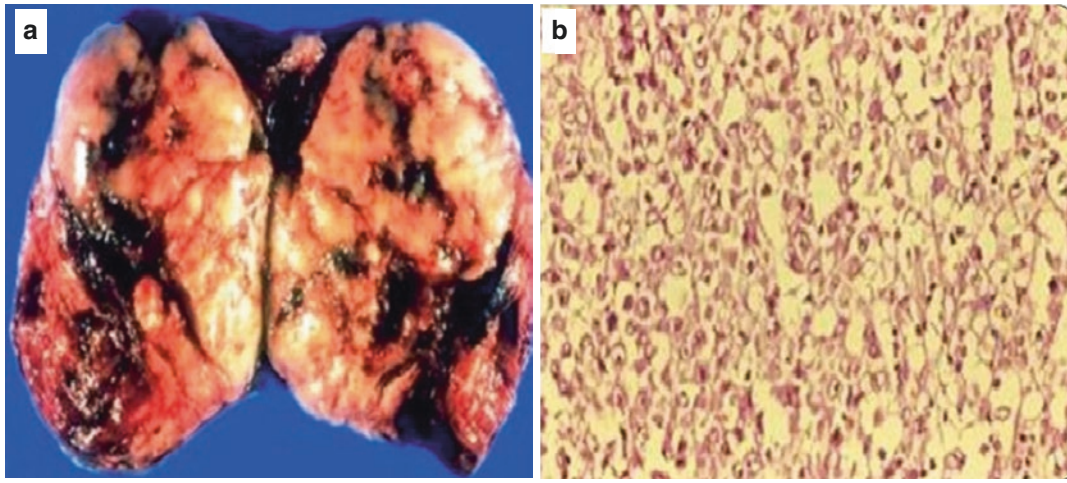

Fig. 39.4 (**a**) Gross specimen of a child with RTK. Cut surface shows large areas of necrosis and hemorrhage. (**b**) Light microscopy (4×) showing sheets of monotonous cells with prominent nucleoli

Table 39.1 Dosage and duration of UH-1 and UH-2

Drugs	Cumulative doses mg/m^2 UH-1	Cumulative doses mg/m^2 UH-2
Cyclophosphamide	14,800	14,800
Carboplatin	3000	3000
Etoposide	2000	2000
Doxorubicin	225	225
Vincristine	**22.5**	**31.5**
Irinotecan	**0**	**60**
Duration (weeks)	**28**	**40**

The current Children's Oncology Group (COG) protocol, ARENO321, recommends intensive ChT with alternating cycles of CTX, carboplatin (CARB), and etoposide (ETOP) alternating with VCR, DOX, and CTX and higher doses of XRT to flanks (20 Gy) for MRTK [17]. In the current COG study trial, children with stage I and II MRTK are treated by revised UH-1 ChT protocol for 28 weeks, while those with stage III and IV would receive vincristine and irinotecan "window" followed by revised UH-2 ChT for 40 weeks [17]. The salient differences between revised UH-1 and UH-2 are as shown in Table 39.1.

MRTK carried a dismal prognosis with overall mortality of 80% at 12–18 months follow-up [16]. An OS of 23.2% at 4-year follow-up was noted in NWTS trial [16]. Moreover, infants less than 6 months of age had worse prognosis than those who were older than 2 years at presentation with 4-year survival being 8.8% and 41.6%, respectively [16]. Even after complete tumor resection with tumor-free margin and negative lymph node (LN) status, only 50% survived with conventional ChT used for WT. [16] Results of current COG protocol, ARENO321, are still awaited.

39.3 Clear-Cell Sarcoma of the Kidney

39.3.1 Incidence and Epidemiology

CSSK is the second most common primary pediatric renal malignancy after WT, accounting for 5% of all renal tumors in childhood [18, 19]. Its diverse histological patterns often

mimic other renal tumors and result in misdiagnosis in 27–50% of patients with CCSK [18, 20]. Historically, it was considered as an unfavorable variant of WT till 1970, when it was identified as a distinct clinicopathological entity [19]. Alike WT, it typically presents in 2–3 years of age with mean age at presentation being 36 months [19, 20]. However**, its more aggressive biological behavior, tendency for late relapses and recurrences, propensity for skeletal and brain metastasis, absence of familial associations and syndromes, and absence of associated nephroblastomatosis are quite unlike WT** [21]. While Marsden et al. termed it as the "bone metastasizing tumor of childhood," Beckwith and Palmer called it "clear-cell sarcoma" based on its histological appearance [19]. Although occasional reports of in utero presentation, in adults as late as 58 years are available, it is extremely rare in first 6 months of life and in adults [19]. Unlike WT, it shows male preponderance of 2:1 and barely occurs bilaterally with only handful of case reports [22].

39.3.2 Clinical Presentation

It is similar to WT with abdominal mass, distension, and hematuria. Other constitutional symptoms like fever, vomiting, anorexia, bony pain, and hypertension can also occur, warranting differentiation from neuroblastoma (NB). CCSK mostly presents with locally advanced disease (stage II: 33%; stage III: 34%), with stage I (27%), stage IV (6%), and bilateral tumors (stage V) being extremely uncommon with few anecdotal reports [18]. LNs are the most frequent site of metastases (51%), followed by bone (13%), lung (10%), and liver (9%). Unlike WT, vascular extension into the renal vein and IVC is unknown in CCSK with only few case reports [23]. It is worthwhile to know that not all renal tumors with vascular thrombosis are WT and an alternate histological diagnosis like CCSK needs to be considered if the tumor and thrombus are not responding to conventional ChT [23]. Vascular thrombus in CCSK is often nonadherent to vessel wall and can be excised [23]. However, sometimes it may require extensive procedures even amounting to cardiopulmonary bypass (CPB) [23]. **Other pathognomonic characteristic of CCSK is its propensity for late relapses in 20–30% of children with CCSK, often occurring at a median time interval of 24 months (range: 5 months to 8 years after completion of treatment**) [18, 19, 21].

Although 30% of relapses occur more than 3 years after diagnosis, it may even occur as late as 10 years, emphasizing the need for long-term follow-up. Conventionally, the bone was the most common site of relapse in CCSK, followed by the lungs, brain, retroperitoneum, and liver. However, with the recent use of intensive ChT protocols, the brain being a safe sanctuary for tumor cells has surpassed the bone as the most common site of CCSK recurrences. Thus, recent recommendations suggest inclusion of drugs with CNS penetration such as ifosfamide in the ChT protocols and emphasize the need for regular brain imaging during follow-up visits [18]. Thus, CCSK is often a diagnosis of exclusion, and its possibility should be entertained if the intrarenal mass is not responding to conventional ChT of Wilms' tumor (WT) [24].

39.3.3 Radiological Diagnosis

Imaging features of CCSK are common to other renal neoplasm. USG usually shows inhomogeneous pattern of soft tissue echoes and well-defined echo-free areas corresponding to tumor necrosis. On CECT, tumors are usually unilateral having well-demarcated soft tissue component with interspersed necrotic areas and calcification in 25% of cases (Fig. 39.5). Clinically, apparent bone and brain metastasis may be absent at the time of initial diagnosis. However, bone scans and brain imaging form an integral part of initial evaluation and follow-up of children with CCSK [25].

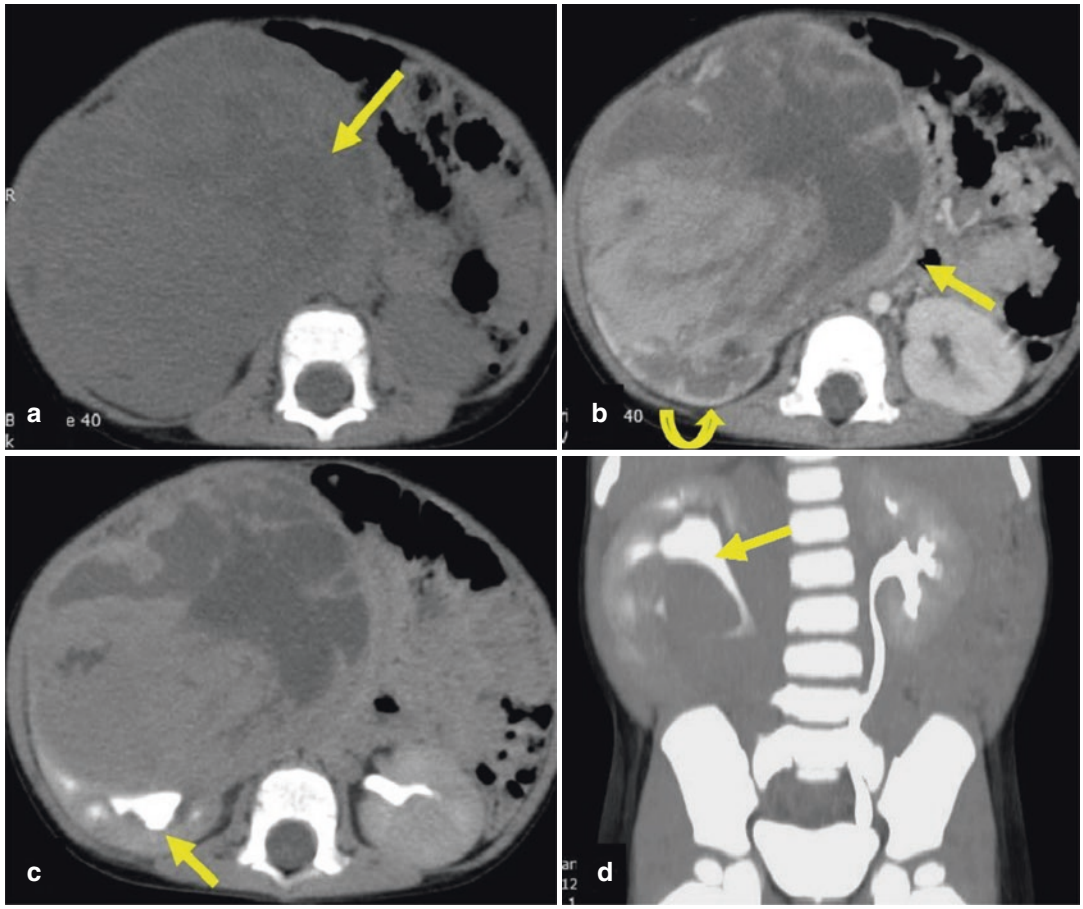

Fig. 39.5 CT scan of a 1.5-year-old child clinically suspected of WT. (**a**) NCCT axial image shows a large solid mass in the right renal fossa with necrotic areas (arrow), with no calcification or hemorrhage. (**b**) CECT axial image reveals a large, heterogeneously enhancing mass arising from lower pole of the right kidney replacing most of the kidney and causing leftward displacement of IVC (arrow) and bowel loops. Mass shows extensive necrosis and enhances less than adjacent renal tissue (elbow arrow). Delayed scans (**c**) axial and (**d**) 3D coronal reformatted image show upward displacement of renal the pelvis (arrow). Histopathology was consistent with CSSK. Bone scan of the child done postsurgery was normal

39.3.4 Pathology

Histopathological diagnosis of CCSK is quite challenging due to diverse histological patterns and mimics other pediatric renal neoplasms. **The useful dictum is that if multiple patterns coexist within the same renal tumor, then one should entertain the diagnosis of CCSK** [21]. On gross examination, it is usually a large, unicentric, well-circumscribed tumor with well-defined margins (Fig. 39.6). On cut section, it has soft tan-gray color and produces abundant mucinous material that imparts a glistening look to it. Cyst, hemorrhage, and necrosis may be present. Errors in histological diagnosis do occur in 27–50% of children with CCSK due to diverse histological patterns [18]. Different patterns may coexist within the same tumor in different proportions. The most common pattern found in CCSK is the classic pattern which may occur diffusely or at least focally in 90% of tumors. It comprises of sheets of cells that are separated by delicate fibrovascular septa with pathognomonic **chicken wire appearance**. The cells contain clear cytoplasm, monotonous round "**Orphan Annie"** nuclei with fine chromatin and indistinct nucleoli (Fig. 39.6).

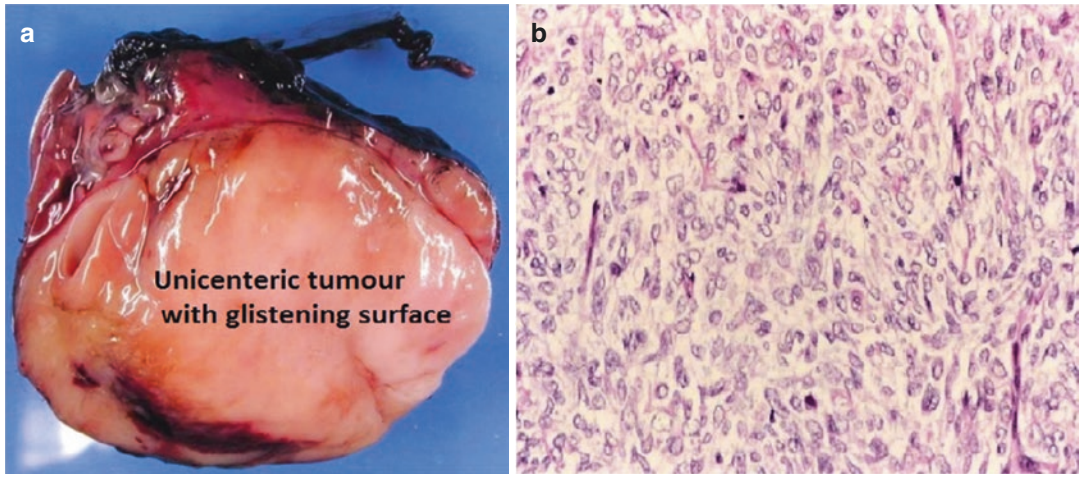

Fig. 39.6 (**a**) Gross specimen of CCSK showing unicentric, well-circumscribed mass with well-defined edges and glistening cut surface. (**b**) Photomicrograph of classical pattern of CCSK showing sheets of cells with "Orphan Annie" nuclei with intervening arborizing septa

The classic pattern closely mimics the blastemal component of WT. Entrapped renal tubules may be visible at the periphery of the tumor creating diagnostic confusion with epithelial component of WT. The interspersed matrix is composed of mucopolysaccharides which contribute to clear-cell appearance [18–21].

Alterations in the cord cell and septal morphology result in a variety of histological patterns in CCSK, namely, myxoid, sclerosing, cellular, epithelioid, spindle, palisading, and anaplastic. Myxoid pattern is observed in 50% of specimens. It is characterized by presence of extracellular myxoid material which comprises of hyaluronic acid and is stained by Alcian blue stain. Sclerosing pattern is seen in one-third of cases (35%) and has acellular deposition of collagen that may get hyalinized to give it an osteoid appearance. Cellular pattern (26%) mimics closely primitive neuroectodermal renal tumors and blastemal component of WT. Palisading and spindle morphology may be confused with cellular variant of CMN. However, CCSK lacks characteristic t(12;15) translocation of CMN [18–21]. FNAC may be needed in children with advanced CCSK who require preoperative ChT. **Varying proportion of cells with clear cytoplasm, septa with arborizing vasculature, and relevant IHC staining may clinch the diagnosis of CCSK** [19].

Recent advances in IHC and molecular genetics had helped immensely in making the precise diagnosis of CCSK. It shows positivity to nonspecific IHC markers like nerve growth factor, vimentin, and Cyclin D1 and is conspicuously negative for WT1, desmin, and cytokeratin. Recently, diffuse strong nuclear positivity **with BCL-6 coreceptor antibody (BCOR)** had provided a sensitive and specific marker for diagnosing CCSK [21]. The two specific genetic events associated with CCSK and of diagnostic significance are recurrent BCOR intrarenal tandem duplication (seen in 70% of CCSK patients) and chromosomal translocation t (10;17) (q22;p13) resulting in fusion of **YWHAE gene with NUTM2B or NUTM2E gene** (observed in 12% of CCSK patients) [21]. Triphasic WT is usually not confused with CCSK. Diagnostic dilemmas arising between blastemal component of WT and CCSK are resorted by strong nuclear positivity of Cyclin D1 in CCSK and its negativity in WT. Similarly, WT1 is positive in WT and negative in CCSK [18, 21].

39.3.5 Management

Over the years, the management of CCSK has evolved and is currently based on risk stratification of the disease. Some landmark recommendations, over the past few decades, that have improved the survival in CCSK include [19, 20]:

(a) Addition of DOX to VCR and AMD.
(b) Addition of CTX to the adjuvant ChT protocol.
(c) Acknowledging brain relapses in CCSK and considering drugs with CNS penetration like ifosfamide (IFO).
(d) Risk stratification of CCSK with treatment of stage I disease with three drugs (VCR, AMD, and CTX) and no postoperative flank XRT in comparison with four-drug protocol (VCR, AMD, CTX, and ETOP) for stage II–IV disease with XRT.

39.3.6 NWTS/COG Protocol

Prior to NWTS-5 (1995–2002), children with CCSK were treated similar to WT. NWTS-5 advocated that all patients diagnosed with CCSK irrespective of the stage undergo primary surgery (radical nephroureterectomy), if possible safely, followed by postoperative ChT (Regimen I) and XRT (10.8 Gy) for 24 weeks [20]. Regimen I included vincristine, doxorubicin, and cyclophosphamide alternating with cyclophosphamide and etoposide. Five-year EFS and OS of 79% and 89%, respectively, were reported with relapse rate of 19% [20]. **AREN0321** (2006–2013) is the current COG protocol recommended for all high-risk pediatric renal tumors including CCSK. Primary surgery (RN with LN sampling) may be done in resectable tumors; otherwise, neoadjuvant ChT may be given for 6 weeks [20]. Postoperative adjuvant ChT for stage I–III is ETOP-CTX-VCR-DOX (ECVD); for stage IV, CARB is added to the ECVD (ECVDC). Postoperative XRT (10.8 Gy) is administered in stage II–IV. Results of this trial are still awaited [20].

39.3.7 SIOP Protocol

During the period 2001–2016, preoperative ChT, AMD, and VCR for stages I to III and AMD, VCR, and DOX (AVD) for stage IV were recommended for 4–8 weeks. This was followed by surgery and postoperative adjuvant ChT for 36 weeks (AVD for stage I and DOX, ETOP, CTX, and CARB for stages II–IV). XRT 25.2 Gy was administered postoperatively in case of stage II and III. Five-year EFS and OS of 78% and 86%, respectively, and relapse rate of 15% were reported [20]. The recently recommended **Umbrella protocol i**s similar to the previous SIOP protocol as far as preoperative ChT is concerned. However, all patients irrespective of the stage receive ETOP, CARB, IFO, CTX, and DOX **(ECICD)** along with 10.8 Gy flank XRT in stage II–III [20]. Results of this trial are also still awaited [20].

39.4 Renal Cell Carcinoma

39.4.1 Incidence and Epidemiology

Pediatric renal cell carcinoma (RCC) poses a unique therapeutic challenge not only due to its rarity but also because of its limited understanding. Majority of inferences on pediatric RCC are drawn either based on small case series or by extrapolating data from adult RCC guidelines. The natural history of pediatric RCC clearly shows its distinct clinical and biological behavior, which is indeed different from adult RCC. It constitutes 2–5% of all pediatric renal neoplasms, and overall only 0.5–2% of all RCC occurs in less than 21 years of age [8, 22, 26]. Mean age at presentation in most series varies from 9 to 15 years (median: 9 years) with no sex predilection [8, 22, 26]. Probability of having a RCC increases with age, and in the second decade of life, WT and RCC have equal chance of occurrence [26, 27]. **RCC should be suspected in a child with renal tumor who presents beyond 5 years of age** [8]. It appears to arise from the epithelium of proximal renal tubules. Furthermore, RCC can

occur as a second malignancy in children after treatment of NB, acute lymphoblastic leukemia, supratentorial PNET, acute non-myelocytic leukemia, and cardiac leiomyosarcoma and after exposure to CTX and topoisomerase inhibitors [28]. Exposure to asbestos, tanning, smoking, obesity, and analgesic overuse are known predisposing factors for adult RCC; however, their association with pediatric RCC is not well-established [27].

39.4.2 Clinical Presentation

Unlike adult RCC, which often presents with metastatic disease, or with paraneoplastic phenomenon (like fever, hypertension, weight loss, hepatic dysfunction, polycythaemia, gynecomastia, and hypercalcemia), pediatric RCC usually presents with one or the other symptoms or signs related to primary tumor (mass, flank or abdominal pain, and hematuria) [8, 27]. Paraneoplastic phenomenon is infrequent in children (5–6%), except an occasional report where it was noted in 31% [27]. Metastasis at presentation to the lung, bone, liver, and brain is identified in 20% of children with RCC [8]. The classic **Grawitz triad** of pain, lump, and hematuria is evident in only 9% of children with RCC [29]. Incidental diagnosis on renal imaging occurs in 50–66% of adult RCC patients, while it is 12–25% in pediatric RCC [8, 30]. Bilateral presentations are rare and are associated with underlying conditions like von Hippel-Lindau disease and tuberous sclerosis [22].

39.4.3 Radiological Diagnosis

RCC presents as solid intrarenal mass with no pathognomonic imaging findings to differentiate it from WT. However, **it is more vascularized and calcification is more common in RCC as compared to WT (25% versus 9%)** (Fig. 39.7) [8]. LN metastases are common and occur even with small primary tumors (<7 cm) [26]. Sensitivity of imaging findings to detect LN metastases in RCC remains low at 57.1%, and imaging alone is not sufficient to rule out nodal involvement in pediatric RCC [26]. It is noteworthy that nearly one-third of the LNs more than 1 cm in size on imaging had positive disease on pathology [26]. Therefore, irrespective of imaging findings, routine LN sampling at surgery is mandatory in pediatric RCC to avoid incomplete staging and better disease control [26].

39.4.4 Pathology

On gross pathological examination, pediatric RCC are smaller in size and have golden yellow appearance as compared with fleshy appearance in WT [8]. Traditionally, RCC exhibits various histological subtypes, namely, conventional or clear-cell carcinoma and papillary. Adult RCC usually have clear-cell, non-papillary histology with translocation or terminal deletion of chromosome 3 at 3p13 [28]. This cytogenetic abnormality at 3p is seldom observed in pediatric RCC, who have translocation involving X chromosome at Xp 11.2 resulting in fusion of TFE3 gene and less commonly TFEB gene at 6p21 to a variety of targets in 24–70% of patients, often labeled as **translocation morphology** [28]. Fusion targets of TFE3 include PRCC, ASPL, PSF, and CLTC [28]. Children with translocation morphology have indolent disease with good outcome and may be amenable to targeted therapy by tyrosine kinase inhibitor in the near future [28, 30]. Translocation morphology is present in 46.7% of pediatric RCC, followed by papillary (16.7%) (Fig. 39.8) [26].

The salient clinical, imaging, and biological differences of pediatric RCC from WT and adult RCC are as shown in Table 39.2 [27, 28].

39.4.5 Management

Surgery is the mainstay of treatment and results in cure if tumor is localized and completely resected. They are ChT and XRT resistant. Most of the children with localized RCC undergo radical nephrectomy with LN sampling [26]. Although debate on LN dissection in RCC con-

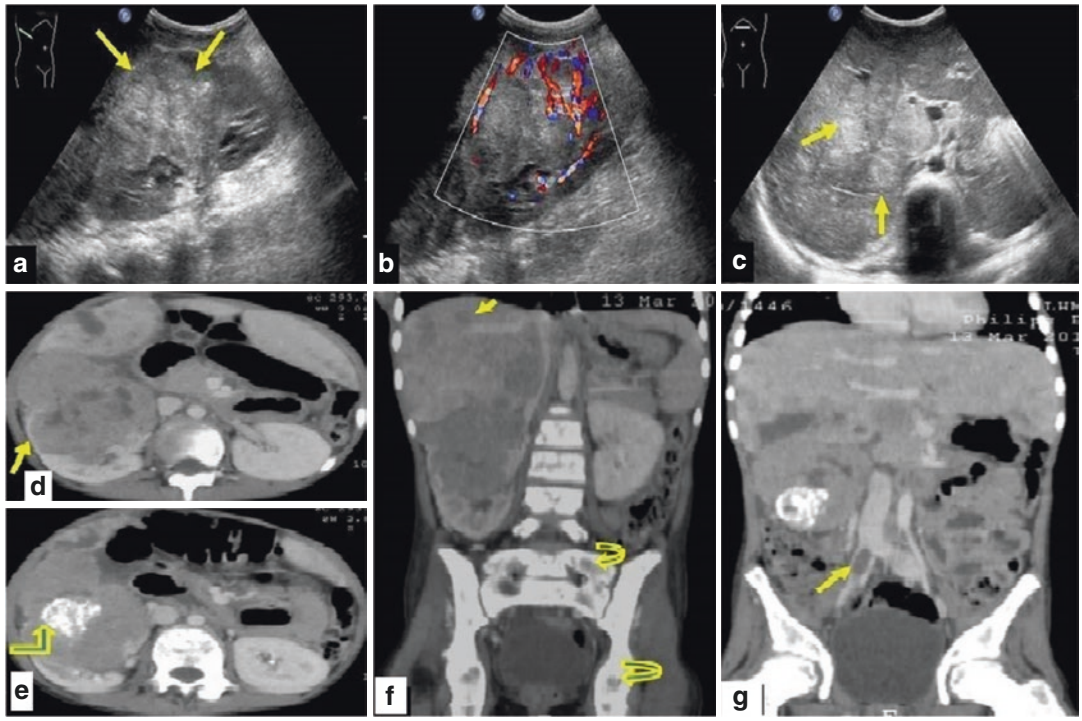

Fig. 39.7 RCC in a 12-year-old male with right flank mass since 5 months. (**a**, **b**) USG gray scale and color Doppler images show a large heterogeneous, hyperechoic lobulated mass with peripheral and internal vascularity arising from interpolar region of the right kidney. (**c**) USG image of the liver shows multiple variable size hyperechoic metastases (arrows). CECT (**d**, **e**) axial images show heterogeneously enhancing mass arising from interpolar region of the right kidney, forming positive beak sign with renal parenchyma (arrow). Mass contains areas of necrosis and coarse, chunky calcification (bent arrow). Coronal multiplanar reformation (MPR) images show (**f**) multiple liver (arrow) and skeletal metastases (curved arrows). (**g**) Non-enhancing hypodense thrombus in the right common iliac vein (arrow)

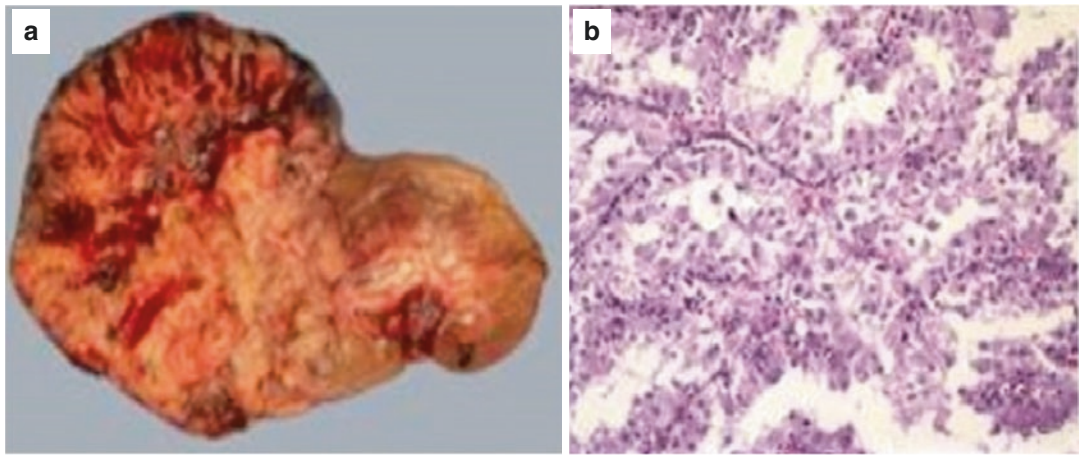

Fig. 39.8 (**a**) Gross morphology of a case of translocation Xp11.2 RCC. (**b**) Light microscopy (4×) showing papillary structure with fibrovascular stalk. Cells have abundant cytoplasm with centrally placed nuclei

Table 39.2 Clinical, imaging, and biological differences of adult RCC, pediatric RCC, and WT

Features	Adult RCC	Pediatric RCC	WT
Mean age (years)	50–60	9–15	2–3
Sex (M:F)	2:1	1:1	1:1
Presentation			
Asymptomatic (%)	50–66	12–36	–
Abdominal lump (%)	32	9–64	90
Hematuria (%)	65	30–50	10
Paraneoplastic syndrome	Frequent	5–6%	Rare
Hypertension (%)	20	5	20
Bilateral (%)	1	10	5
Calcification on imaging (%)	5	24	5–10
Histology	Mixed, clear cell	Translocation, papillary	Triphasic, biphasic, monophasic
IHC	3p translocation	TEF3	WT1, WT2

tinues, recent evidence supports mandatory LN sampling in all pediatric RCC [26]. For left-sided RCC, hilar, paraaortic, and ipsilateral common iliac nodes and for right-sided RCC, hilar, inter aortocaval, retrocaval, and ipsilateral common iliac nodes should be sampled [28]. Nephron sparing surgery (NSS) was resorted to in 15% of pediatric RCC with lower tumor stage [26]. However, their role is not well-established in the management of pediatric RCC. For advanced metastatic disease with unresectable RCC, the management options are limited. Immunotherapy with interferon and interleukin (IL_2), tyrosine kinase inhibitors like sunitinib, rapamycin, and platinum-based ChT may be tried in these children [22]. The 5-year OS of pediatric RCC is better than adult RCC (60% and 40%, respectively) [27]. Pediatric RCC with stage I–III have 100% and stage IV have less than 10% 5-year survival [27].

39.5 Intrarenal Neuroblastoma

Intrarenal neuroblastoma (IRNB) are rare, aggressive renal neoplasm, which may mimic clinical and imaging features of WT. Their biological behavior and prognosis is however very different from WT. They usually arise from adrenal nests located within the renal tissue or from the intrarenal sympathetic ganglia and need to be differentiated from secondary intrarenal invasion by a malignant suprarenal mass [31, 32]. Unlike WT, they occur in younger age group (11–40 months) with occasional reports in older children [32]. They are usually associated with constitutional symptoms like fever, weight loss, anemia, and bony pains. The renal mass is usually indistinguishable from that of WT, though it often crosses midline. **An important clinical clue to their diagnosis is the presence of associated hypertension in nearly 66–100% of children with IRNB as compared to 20% in WT and 27% in extrarenal NB** [33]. Catecholamine release from the tumor and compression of renal artery by the tumor with secondary renin angiotensin system activation lead to hypertension. Majority of them (80%) may present with metastases to the bone, bone marrow, and lymph nodes [32, 33]. Although their imaging findings mimic WT, presence of vascular encasement, massive retroperitoneal lymphadenopathy, and intrarenal speckled, multifocal, ringlike calcification is seen more frequently in IRNB (40–67%) as compared to WT (13%) [32–34]. Thus, the possibility of IRNB should always be kept in a child presenting with a renal mass presenting with hypertension, multifocal intrarenal calcification, and evidence of vascular encasement on imaging (Fig. 39.9). Assessment of urinary catecholamine levels, MIBG scans, and bone marrow aspiration may clinch the diagnosis in such patients. Management consists of cisplatin-, adriamycin-, and cyclophosphamide-based ChT with RN with adrenalectomy.

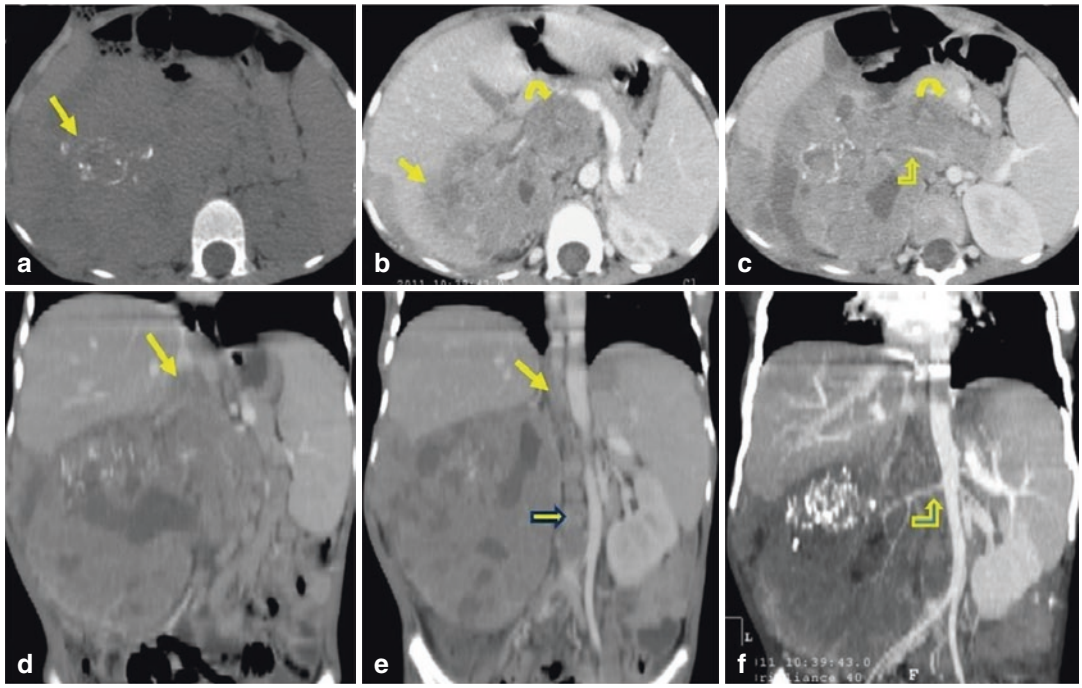

Fig. 39.9 IRNB in a 6-year-old male child with abdominal distension and malaise. CT scan axial images NCCT (**a**) show a mass in the right renal fossa with calcification (arrow); CECT (**b**, **c**) show right renal mass with calcification, adjacent liver infiltration (arrow), encasement of the right renal artery (bent arrow), thrombosis of the right renal vein, and IVC (curved arrow) with extension into the left renal vein. Coronal MPR images (**d**, **e**) show malignant tumor thrombus in IVC (arrow) and retroperitoneal lymphadenopathy (block arrow). Coronal maximum intensity projection (MIP) (**f**) shows right renal artery encasement (bent arrow) by the mass. Based on imaging features, diagnosis of WT was suggested. However, histopathology showed small round cells in a fibrillary background suggestive of NB. Urinary vanillylmandelic acid (VMA) was raised

39.6 Primitive Neuroectodermal Tumor (PNET) or Renal Ewing's Tumor

They arise from neural crest cells and neuroectoderm and are usually located in the paraspinal area and ribs and rarely from the skin, soft tissues, kidney, and retroperitoneum [35]. Unlike osseous Ewing's sarcoma, which occurs at a median age of 15 years, renal Ewing's tumor occurs in adolescents or young adults [35]. **It is primarily a histological diagnosis** with nonspecific clinical presentation. One-third of the patients have metastasis and vascular thrombus at presentation [36]. It is composed of primitive round blue cells with high nuclear cytoplasmic ratio and **perivascular pseudo-rosette formation** (Fig. 39.10). IHC staining and molecular studies play a key role in establishing the accurate diagnosis. A panel of IHC markers including CD99, NSE, WT1, LCA, FL-1, cytokeratin, desmin, myogen, and chromogranin are usually required to ensure precise diagnosis [37]. **While renal PNET are positive for CD99, NSE, and FL-1, they are negative for the rest of the IHC markers.** They also exhibit translocation t (11;22) (q24; q12) with fusion of EWS-FIL-6 gene [37]. They require multimodal therapy including induction ChT with VCR, IFO, DOX, and ETOP **(VIDE)** for six courses followed by local control by RN and consolidation ChT with VCR, AMD, and IFO (VAI) for standard-risk patients and VAI plus high dose busulfan and melphalan for high-risk patients [37]. Local XRT

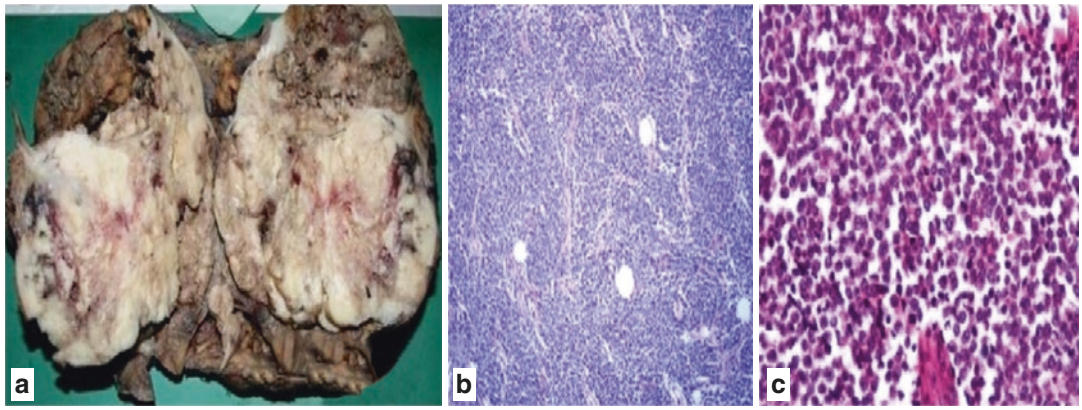

Fig. 39.10 (**a**) Gross examination showing a friable, grayish white, lobulated mass (15 × 13 × 7 cm), with multiple foci of hemorrhage and necrosis replacing most of the kidney. (**b**) Tumor composed of monotonous sheets of round cells divided by fibrovascular septae. (**c**) Focal areas of pseudo-rosette

may be administered for incomplete resection or with PTMs. Five-year OS is dismal (45–55%) [37].

39.7 Renal Lymphoma

Renal involvement in lymphoma usually occurs due to systemic spread of non-Hodgkin's lymphoma (Burkitt's subtype) manifesting as multiple or solitary metastatic nodules or infiltrates in kidney [38]. Primary renal lymphoma (PRL) is extremely rare and is thought to arise from mucosa associated lymphoid tissue [39]. Specific diagnostic criteria laid down for diagnosing PRL emphasize on absence of other nodal or extranodal involvement. PRL usually presents with renal enlargement which may be bilateral in 10–20% of patients [39]. It may even present with renal failure and hypertension [38]. Multiple bilateral renal masses on imaging as seen in renal lymphoma are also noted in WT, cystic renal tumors, angiomyofibroma, metastatic disease, acute myeloid leukemia, and fungal infection [39]. **Although renal lymphoma does not have any characteristic imaging finding, retroperitoneal lymphadenopathy with involvement of the liver and spleen may suggest its diagnosis**. They are classically described as homogeneous masses, but they may have heterogeneous attenuation as shown in Fig. 39.11.

Renal failure in lymphoma is multifactorial and can be due to vascular or ureteric obstruction by the engulfing renal mass or by enlarged retroperitoneal LNs and rarely due to tumor associated glomerulopathy [38]. Renal failure is often aggravated by induction ChT with rapid breakdown of tumor cells leading to hyperuricemia (>8 mg %), hyperphosphatemia (≥6.5 mg%), hyperkalemia (>6 mg%), uremia, and hypocalcemia (<7 mg%) [40]. These metabolic derangements, collectively termed as **tumor lysis syndrome**, occur due to massive destruction of tumor cells with release of nucleic acids, electrolytes, and cytokines in systemic circulation. It poses a medical emergency with risk of cardiac arrhythmia, renal failure, seizures, coma, and sudden death [40]. Management usually involves prophylactic intravenous hydration, electrolyte correction, use of hypouricemic agents like allopurinol and rasburicase, and dialysis if required [40]. Management of renal lymphoma is usually medical with use of drugs like VCR, prednisolone, CTX, L-asparaginase, and cytosine arabinoside as in NHL [38].

39.8 Angiomyolipoma

Angiomyolipoma (AML) is an extremely rare benign mesenchymal renal tumor constituting less than 0.3% of all renal tumors [41]. It was

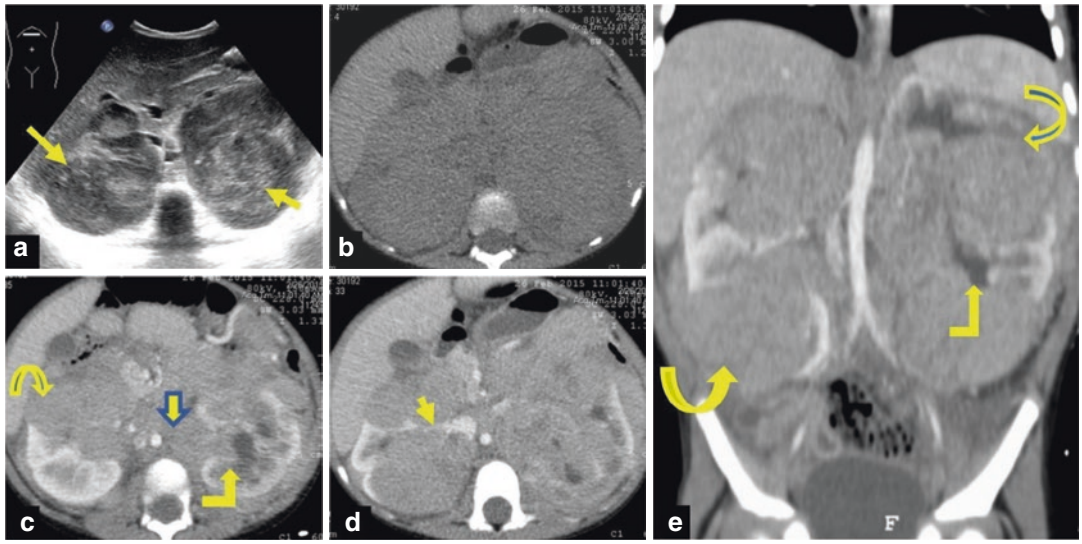

Fig. 39.11 Bilateral primary renal Burkitt's lymphoma in a 4-year-old male child with on and off fever, abdominal pain, and distension. USG abdomen transverse view (**a**) shows bilateral enlarged kidneys with multiple hypoechoic and hyperechoic lesions and loss of corticomedullary differentiation. Axial NCCT (**b**) and CECT (**c**, **d**, **e**) scan images show multiple large ill-defined round to oval heterogeneously enhancing lesions (curved arrows) in bilateral renal parenchyma distorting the renal contour, encasing renal vessels (arrow), splaying and encasement renal pelvis, and calyces (bent arrow). Enlarged preaortic and paraaortic LNs are seen (block arrow)

initially considered to be hamartoma consisting of mature adipose tissue, dysmorphic blood vessels, and smooth muscles; later, however, it was evident that it arises from perivascular epithelioid cells and was designated as PECOMA [41, 42]. Majority of AML (80%) occur sporadically in adult females, without associated genetic syndromes, and are diagnosed incidentally on imaging studies [41, 42]. However, remaining 20% of them have associated tuberous sclerosis (TSC) or lymphangioleiomyomatosis (LAM). TSC is an autosomal dominant disease characterized by subependymal nodules and astrocytoma manifesting as epilepsy, neurocognitive impairment, and autism and may be associated with hypomelanotic macular skin lesions, facial angiofibroma, and ungal fibroma [41]. LAM is a rare condition where there is smooth muscle infiltration into the small airways and alveoli leading to degenerative changes and respiratory failure [42]. Unlike sporadic AML, which are usually unilateral, those with TSC occur at early age, within the first decade of life, and are often large, multifocal, and bilateral [41, 42]. **Therefore, in all newly diagnosed cases of pediatric AML, it is mandatory to have a formal work-up for TSC, and genetic counseling is advisable**. Surprisingly, however, there are numerous reports of non-TSC, sporadic AML in children as young as 13 months of age presenting as unilateral tender, renal masses associated with a history of trivial trauma, acute flank pain, hematuria, and hypertension being often mistaken as WT or RCC [43, 44]. Retroperitoneal hematoma (**Wunderlich syndrome**) and hemorrhagic shock due to tumor rupture are some of the other rare life-threatening presentations of AML [42].

The pathognomonic distinguishing feature of AML from other renal neoplasms is the presence of fat in the lesion as shown in Fig. 39.12 [41–44]. Tissue attenuation values of <−10 Hounsfield unit (HU) on NCCT are suggestive of fat [42]. A subset of **fat-poor** or **minimal-fat AML** (4–5%) pose a diagnostic dilemma and need to be differentiated from RCC [44]. Although presence of peritumoral collateral blood vessels, calcification, and claw-sign are suggestive of RCC, but in equivocal cases, further clarity on diagnosis may be provided by either "chemical shift MRI" or percutaneous biopsy [42, 44]. Histologically,

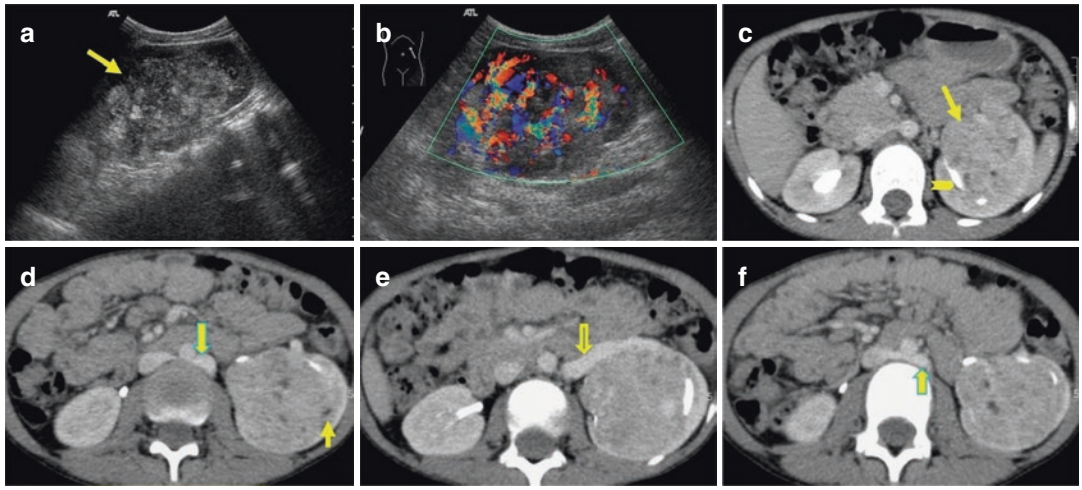

Fig. 39.12 Eight-year-old male child, a known case of tuberous sclerosis, presented with left flank pain and renal mass. USG abdomen (**a**, **b**) shows a heteroechoic left renal mass with non-shadowing echogenic areas (fatty elements) and marked internal vascularity. CECT scan images (**c**) show heterogeneously enhancing left renal mass (arrow) distorting the calyces (arrowhead). (**d**) Mass shows multiple small hypodense foci (small arrow) of fat attenuation and retroaortic course of left renal vein (block arrow). (**e**, **f**) A dilated venous channel (block arrows) was extending from the mass, with retroaortic course, draining into IVC

there are two main types of AML, a classical type and an epithelioid variant; both show **positive immunostaining with HMB 45.** Most of AML are benign and have nominal risk of malignancy with vascular invasion and perirenal extension. LN metastases are reported with large tumors (>7 cm) of epithelioid histology [41, 42].

Management is usually conservative with annual USG surveillance if the tumor is small (<4 cm). Surgical resection may be required in large tumors (>4 cm) especially if they are symptomatic and are prone to rupture as suggested by associated aneurysm >5 mm [41]. Any suspicion of malignancy and inability to have regular follow-up also warrant surgical resection. NSS is advocated in children with low nephrometric scoring or in setting of TSC with bilateral renal involvement [41, 45]. Predominately exophytic masses and polar distribution, at least 7 mm or more away from renal sinus and pelvicalyceal system, have low nephrometric scores and are thus more amenable for partial nephrectomy [45]. Selective arterial embolization (SAE) with gelatin microspheres and absolute alcohol, cryoablation, and radiofrequency ablation (RFA) are some of the novel treatment options for AML with a success rate of 60–89% [41]. In bulky, unresectable tumors and in those with limited renal reserve, mTOR inhibitors like sirolimus, rapamycin, and more recently everolimus have been used with 30% response in 80% of cases [41].

39.9 Renal Cystic Tumors

Renal cystic tumors may present with a wide spectrum of lesions ranging from cystic nephroma and cystic partially differentiated nephroblastoma (CPDN) to cystic variant of WT. Cystic nephroma (CN) is a benign lesion, usually presenting as a multilocular cyst in a child. CN is an uncommon tumor with incidence of <1%. It has bimodal age group of presentation, first peak is seen in <4 years of age with male predominance, and the second peak is seen in adults with female predominance [46, 47]. CPDN, considered as a favorable histology variant of WT, is seen in <2 years of age with male/female ratio of 2:1 [48]. Both CN and CPDN can present with abdominal mass and rarely hematuria [49].

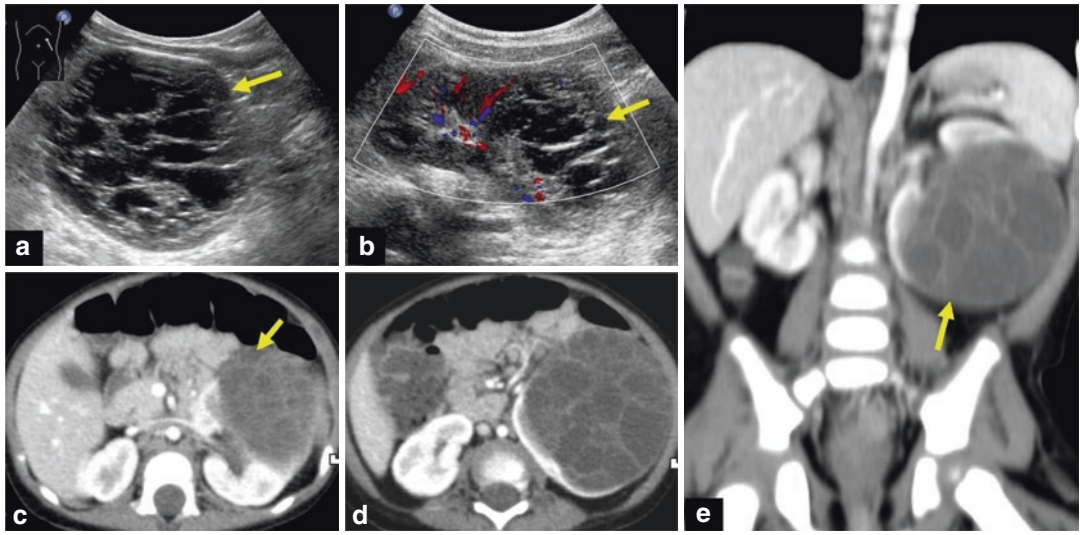

Fig. 39.13 Multilocular CN in a 14-year-girl with nontender left renal lump. USG gray scale and color Doppler images (**a**, **b**) show a well-encapsulated, avascular multilocular cystic mass in the left kidney. CECT images axial (**c**, **d**) and coronal MPR (**e**) show a well-circumscribed multicystic left renal mass with mildly enhancing thin internal septae separating the variable-sized cysts. Mass is arising from interpolar region and lower pole of the left kidney and does not show any septal calcification or enhancing soft tissue

It usually presents as a unilateral, well-encapsulated, solitary multilocular lesion, comprising of multiple noncommunicating cyst of varying sizes (Fig. 39.13); cysts neither communicate with each other nor with pelvis. They may present with flank pain, abdominal mass, urinary tract infection, hypertension, or hematuria. Cysts in multilocular CN are lined by cuboidal epithelium, and the septa are composed of fibrous tissue, in which well-differentiated tubules may be present [50]. The surrounding renal parenchyma may be compressed. While in CPDN, the septa contain blastemal cells with or without epithelial and stromal cell types. Thus, CN and CPDN lack solid component and have similar imaging findings. The distinction between the two is done by histological examination of resected specimen. On the contrary, cystic WT has solid component besides the cyst and has distinct differentiating features on radiology and histology. Both CN and stage I CPDN are managed by nephrectomy alone. Postoperative adjuvant ChT, as in WT, may be needed in higher stages of CPDN [50]. Both CN and CPDN have excellent prognosis with complete surgical excision [46, 48].

39.10 Ossifying Renal Tumor of Infancy

Ossifying renal tumor of infancy is a rare benign tumor arising from papillary region of renal medulla and extends into the collecting system. It occurs in infants with age ranging from 6 days to 14 months. It commonly presents with hematuria and mimics staghorn calculus due to its ossification. On imaging, it usually presents with hydronephrosis with a filling defect in the collecting system [15].

39.11 Metanephric Stromal Tumors

Metanephric neoplasms may sometimes mimic WT. They are rare benign tumors of the kidney and have a wide spectrum ranging from pure epi-

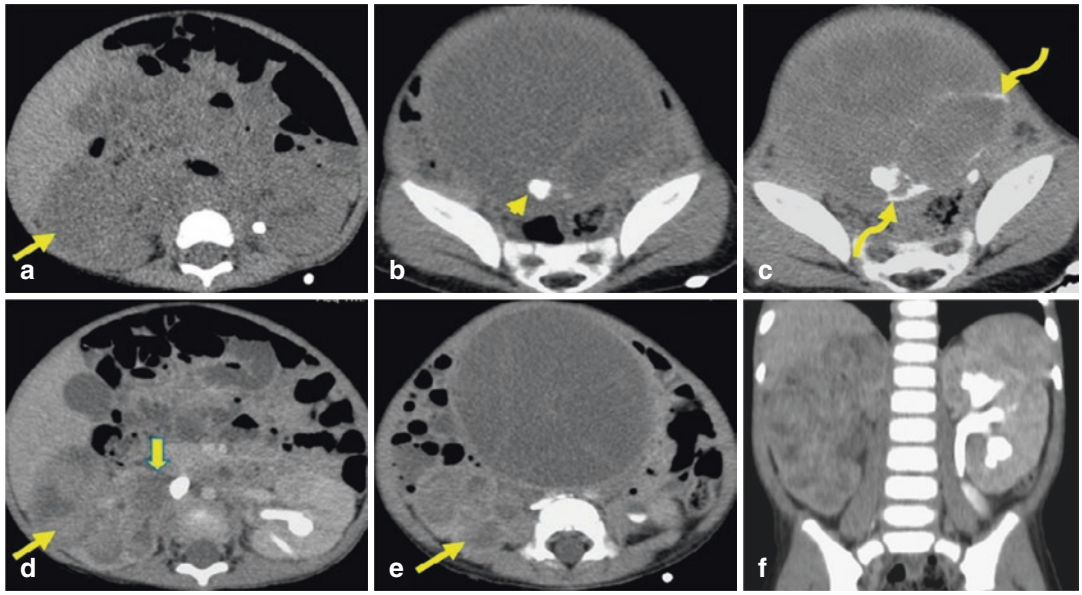

Fig. 39.14 Metanephric stromal tumor in a 2-year-old male child who presented with progressively increasing abdominal distension. NCCT axial images (**a**, **b**) show a hypodense right renal mass (arrow) and a mass with calcification (arrowhead) filling the urinary bladder, causing its distension. CECT axial images. (**c**) Streaks of contrast (curved arrow) seen in urinary bladder, with heterogenous enhancement of the mass. (**d**, **e**) Heterogeneously enhancing mass involving the renal medulla, pelvicalyceal system causing marked parenchymal thinning. Mass is extending into the renal pelvis and ureter (block arrow). Corticomedullary differentiation is preserved in the left kidney. (**f**) Coronal MPR shows mild hydronephrosis and dilated upper ureter secondary to obstruction by the mass. Percutaneous nephrostomy tube is seen in situ in the left renal pelvis

thelial metanephric adenoma to pure stromal variety (metanephric stromal tumors). Metanephric adenofibroma lies in the middle of the spectrum and has both epithelial and stromal components and is easily misdiagnosed as biphasic WT [51]. It is, however, important to differentiate them from WT as surgery is the mainstay of their treatment and they often do not require ChT and XRT [52]. Figure 39.14 displays the imaging findings of metanephric stromal tumor in a patient who had undergone nephroureterectomy.

In conclusion, the most common NWRT in infants include CMN and RTK, whereas RCC predominates in adolescence. CCSK has similar age distribution as WT. Other rare malignant NWRT includes lymphoma, PNET, and IRN. Multilocular CN, CPDN, and AML are some of the common nonmalignant pediatric renal tumors. The diagnosis of NWRT should always be entertained in children less than 6 months and more than 6 years of age, especially when they present with advanced disease and metastasis to the brain, bones, or lungs at a very young age. Imaging features of unencapsulated tumor with retroperitoneal extension to psoas muscle, large extrarenal mass, vascular encasement, large retroperitoneal lymphadenopathy, and abundant calcification in a presumed renal mass should also raise a suspicion of NWRT. As the management and prognosis of these tumors are variable and differ significantly from WT, it is warranted that a histological confirmation should be done at the outset. Use of IHC and molecular genetics has not only reduced the diagnostic uncertainties but has also helped in risk stratification of these tumors. A brief synopsis of NWRT is shown in Table 39.3.

Table 39.3 Synopsis of pediatric NWRT (salient clinical, imaging, and pathological clues to diagnosis)

Tumor	Median age	Diagnostic clues (clinical + imaging)	Pathology/IHC cytogenetics	Treatment/outcomes
CMN	2 months	– Renal lump in neonates, <3 months – Hypercalcemia – Ill-defined edges – Double-rim sign – Intra-tumor pelvis	Classical, cellular, mixed Positive IHC: Vimentin, Actin Trisomy 11 Translocation (t12:15)(p13;q25) ETV6 NTRKS gene fusion	RN with LN sampling Adjuvant treatment: – Incomplete excision – Cellular/mixed histology – Tumor margin positive – Age > 3 months 5-year OS >95%
MRTK	11 months (<4.5 years)	– Large renal lump <1 year – Presentation with advanced disease + metastasis (brain/bone) – Hematuria – Hypercalcemia – Central renal mass, ill-defined edges, into renal sinus+ pelvis – Lobular architecture – Linear calcification	– Monomorphic cells + large nucleus + owl eye nucleoli – Pathognomonic Intracytoplasmic pink Inclusions – INI-1 negative	If resectable- RN+ LN sampling + ChT+ XRT If unresectable—Neoadjuvant ChT for 6 weeks Current COG: Alternating cycle of CARBO, CYCLO, ETOPO (CCE) with VCR, DOX, CYCLO (VDC). (UH-1, UH-2) + XRT in all stages Dismal prognosis
CCSK	36 months	– Aggressive behavior – Presentation as locally advanced disease – Unresponsive to conventional CT of WT – Tendency for skeletal + brain metastases – Late relapse and recurrences – Rarely bilateral – Vascular involvement rare	Multiple patterns in the same tumor – Abundant myxoid material—gives it glistening cut surface – Characteristic Chicken Wire appearance + Orphan Annie nuclei – IHC- cyclin D1+, WT1 negative, BCL6 positive – Translocation of t(10:17)(q22;p13) with fusion of YWHAE gene with NUTM2B	– If resectable, RN+ LN sampling + ChT + XRT (except stage I) – If unresectable, neoadjuvant ChT for 6 weeks Current COG: (Regimen I) ECVD− stage I–III ECVD+ carboplatin—Stage IV XRT− stage II–IV (local + metastasis) 5-year OS—79–89% Relapse rate—19%
RCC	9–15 years	– Suspect RCC in a child with renal mass > 5 years of age – Paraneoplastic 5–6% – More vascularized mass + calcification	– Translocation pathology on Xp.12 – Papillary IHC: TFE3	– RN+ LN sampling – Metastatic: Interferon, IL2, tyrosinase inhibitor like rapamycin, sunitinib 5-year survival: Stage I–III: 100% Stage IV: 10%
IRNB	11–40 months	Suspect in a child with renal mass + hypertension + calcification	Confirmation with urinary catecholamine MIBG Bone marrow	As neuroblastoma

Table 39.3 (continued)

Tumor	Median age	Diagnostic clues (clinical + imaging)	Pathology/IHC cytogenetics	Treatment/outcomes
PNET	Adolescence	Nonspecific	Perivascular pseudo-rosette formation IHC: CD99 +, FL-1 +	Induction ChT (VIDE), local control, postoperative adjuvant ChT (VAI) 5-year OS -45–55%
PRL	Variable	Bilateral renal lumps Bilateral renal infiltrates Retroperitoneal LN Hepatosplenomegaly	As for NHL	As for NHL
AML	Variable	– Sporadic/genetic – Tuberous sclerosis needs to be ruled out – Tender renal lump after trivial trauma – Flank pain, hematuria – Fat density in lesion	Classical, epithelioid IHC: HMB +ve	Observation <4 cm Surgery: NSS >4 cm, symptomatic, prone to rupture Noncompliance to follow-up Large tumor with epithelioid histology SAE, Cryoablation mTOR inhibitors: Sirolimus, rapamycin everolimus
CN/ CPDN	<24 months	Multilocular, noncommunicating cyst	CPDN: Blastemal cells in septa CN: Fibrous septa, may have mature tubules	Surgery: RN CPDN: Relapse/II–IV may need ChT

RN radical nephrectomy, *WT* Wilms' tumor, *IRN* intrarenal neuroblastoma, *RCC* renal cell carcinoma, *CCSK,* clear-cell sarcoma, *MRTK* malignant rhabdoid tumor of the kidney, *CMN* congenital mesoblastic nephroma, *PNET* primitive neuroectodermal tumor, *PRL* primary renal lymphoma, *AML* angiomyolipoma, *CN* cystic nephroma, *CPDN* cystic partially differentiated nephroblastoma, *ChT* chemotherapy, *XRT* radiotherapy, *LN* lymph node, *OS* overall survival

References

1. Bisceglia M, Carosi I, Vairo M, Zaffarano L, Bisceglia M, Creti G. Congenital mesoblastic nephroma: report of a case with review of the most significant literature. Pathol Res Pract. 2000;196:199–204. https://doi.org/10.1016/S0344-0338(00)80101-6.
2. Chen Y, Zhou L, Liao N, Gao P, Chen L, Li X, et al. Specific computed tomography imaging characteristics of congenital mesoblastic nephroma and correlation with ultrasound and pathology. J Pediatr Urol. 2018;14:571.e1–571e6. https://doi.org/10.1016/j.jpurol.2018.07.020.
3. Campagnola S, Fasoli L, Flessati P, Sulfasso M, Balter R, Pea M, et al. Congenital cystic mesoblastic nephroma. Urol Int. 1998;61:254–6. https://doi.org/10.1159/000030342.
4. Jayabose S, Iqbal K, Newman L, et al. Hypercalcemia in childhood renal tumors. Cancer. 1988;61:788–91. https://doi.org/10.1002/1097-0142(19880215)61:4<788::aid-cncr2820610424>3.0.co;2-h.
5. Khashu M, Osiovich H, Sargent MA. Congenital mesoblastic nephroma presenting with neonatal hypertension. J Perinatol. 2005;25:433–5. https://doi.org/10.1038/sj.jp.7211304.
6. Bera G, Das RN, Bisht J, Mishra PK, Mallick GM, Chaudhuri MK, et al. Cytological diagnosis of mesoblastic nephroma: a report of three cases with summary of prior published cases. Diagn Cytopathol. 2016;44:823–7. https://doi.org/10.1002/dc.23519.
7. Chaudry G, Perez-Atayde AR, Ngan BY, Gundogan M, Daneman A. Imaging of congenital mesoblastic nephroma with pathological correlation. Pediatr Radiol. 2009;39:1080–6. https://doi.org/10.1007/s00247-009-1354-y.
8. Ahmed HU, Arya M, Duffy PG, Mushtaq I, Sebire IN. Primary malignant non-Wilms' renal tumour in children. Lancet Oncol. 2007;8:730–7. https://doi.org/10.1016/S1470-2045(07)70241-3.
9. England RJ, Haider N, Vujanic GM, Kelsey A, Stiller CA, Kathy PJ, et al. Mesoblastic nephroma: a report of the United Kingdom Children's cancer and Leukaemia group (CCLG). Pediatr Blood Cancer. 2011;56:744–8. https://doi.org/10.1002/pbc.22871.

10. Jehangir S, Kurian JJ, Selvarajah D, Thomas RJ, Holland AJA. Recurrent and metastatic congenital mesoblastic nephroma: where does the evidence stand? Pediatr Surg Int. 2017;33:1183–8. https://doi.org/10.1007/s00383-017-4149-5.
11. Agrons GA, Kingsman KD, Wagner BJ, Sotelo-Avila C. Rhabdoid tumor of the kidney in children: a comparative study of 21 cases. AJR Am J Roentgenol. 1997;168:447–51. https://doi.org/10.2214/ajr.168.2.9016225.
12. Chung CJ, Lorenzo R, Rayder S, Johnson JE, Navarro OM, Hernanz-Schulman M. Rhabdoid tumors of the kidney in children: CT findings. AJR Am J Roentgenol. 1995;164:697–700. https://doi.org/10.2214/ajr.164.3.7863897.
13. Amar AM, Tomlinson G, Green DM, Breslow NE, de Alarcon PA. Clinical presentation of rhabdoid tumors of the kidney. J Pediatr Hematol Oncol. 2001;23:105–8. https://doi.org/10.1097/00043426-200102000-00007.
14. Han TI, Kim MJ, Yoon HK, Chung JY, Choeh K. Rhabdoid tumour of the kidney: imaging findings. Pediatr Radiol. 2001;31:233–7. https://doi.org/10.1007/s002470000417.
15. Lowe LH, Isuani BH, Heller RM, et al. Pediatric renal masses: Wilms tumor and beyond. Radiographics. 2000;20:1585–603. https://doi.org/10.1148/radiographics.20.6.g00nv051585.
16. Ahmed HU, Arya M, Levitt G, Duffy PG, Sebire NJ, Mushtaq I. Part II: treatment of primary malignant non-Wilms' renal tumours in children. Lancet Oncol. 2007;8:842–8. https://doi.org/10.1016/S1470-2045(07)70276-0.
17. Geller JI. Current standards of care and future directions for "high-risk" pediatric renal tumors: anaplastic Wilms tumor and rhabdoid tumor. Urol Oncol. 2016;34:50–6. https://doi.org/10.1016/j.urolonc.2015.10.012.
18. Aw SJ, Chang KTE. Clear cell sarcoma of the kidney. Arch Pathol Lab Med. 2019;143:1022–6. https://doi.org/10.5858/arpa.2018-0045-RS.
19. Gooskens SL, Furtwängler R, Vujanic GM, Dome JS, Graf N, van den Heuvel-Eibrink MM. Clear cell sarcoma of the kidney: a review. Eur J Cancer. 2012;48:2219–26. https://doi.org/10.1016/j.ejca.2012.04.009.
20. Gooskens SL, Graf N, Furtwängler R, Spreafico F, Bergeron C, Ramirez-Villar GL, et al. Position paper: Rationale for the treatment of children with CCSK in the UMBRELLA SIOP-RTSG 2016 protocol. Nat Rev Urol. 2018;15:309. https://doi.org/10.1038/nrurol.2018.14.
21. Aldera AP, Pillay K. Clear cell sarcoma of the kidney. Arch Pathol Lab Med. 2020;144:119–23. https://doi.org/10.5858/arpa.2018-0353-RS.
22. Broecker B. Non-Wilms renal tumours in children. Urol Clin North Am. 2000;37:463–9. https://doi.org/10.1016/s0094-0143(05)70094-x.
23. Sugandhi N, Murghate G, Malankar DP, Das S, Bisoi AK, Gupta AK, et al. Pediatric clear cell sarcoma of kidney with cavoatrial thrombus. J Pediatr Surg. 2011;46:2387–90. https://doi.org/10.1016/j.jpedsurg.2011.09.050.
24. Kumar P, Kumari P, Sarin YK. Clear cell sarcoma: pitfalls and management. Open Access J Surg. 2018;7:555716. https://doi.org/10.19080/OAJS.2018.07.555716.
25. Glass RB, Davidson AJ, Fernbach SK. Clear cell sarcoma of the kidney: CT, sonographic, and pathologic correlation. Radiology. 1991;180:715–7. https://doi.org/10.1148/radiology.180.3.1871282.
26. Geller JI, Ehrlich PF, Cost NG, Khanna G, Muller EA, Gratias EJ, et al. Characterization of adolescent and pediatric renal cell carcinoma: a report of the children oncology group study AREN03B2. Cancer. 2015;121:2457–64. https://doi.org/10.1002/cncr.29368.
27. Carcao MD, Taylor GP, Greenberg ML, Bernstein ML, Champagne M, Hershan L, et al. Renal cell carcinoma in children: a different disorder from its adult counterpart? Med Pediatr Oncol. 1998;31:153–8. https://doi.org/10.1002/(sici)1096-911x(199809)31:3<153::aid-mpo5>3.0.co;2-a.
28. Sausville JE, Hernandez DJ, Argani P, Gearhart JP. Pediatric renal cell carcinoma. J Pediatr Urol. 2009;5:308–14. https://doi.org/10.1016/j.jpurol.2009.04.007.
29. Rialon KL, Gulack BC, Englum BR, Routh JC, Rice HE. Factors impacting survival in children with renal cell carcinoma. J Pediatr Surg. 2015;50:1014–8. https://doi.org/10.1016/j.jpedsurg.2015.03.027.
30. Young EE, Brown CT, Merguerian PA, Akhavan A. Pediatric and adolescent renal cell carcinoma. Urol Oncol. 2016;34:42–9. https://doi.org/10.1016/j.urolonc.2015.06.009.
31. Sellaturay SV, Arya M, Banisadr S, Murthi GV, Sebire NJ, Duffy PG. Primary intrarenal neuroblastoma: a rare and aggressive tumour of childhood mimicking Wilms tumour. J Pediatr Surg. 2006;2:522–4. https://doi.org/10.1016/j.jpurol.2005.11.010.
32. Kessler OJ, Siegel JF, Brock WA. Intrarenal neuroblastoma masquerading as Wilms tumour. Urology. 1998;51:313–6. https://doi.org/10.1016/s0090-4295(97)00690-0.
33. Farmakis S, Siegel NJ. Intrarenal neuroblastoma with pulmonary metastasis mimicking a Wilms tumour. J Pediatr Surg. 2014;49:1864–6. https://doi.org/10.1016/j.jpedsurg.2014.10.043.
34. Sarin YK, Senagar M. Intrarenal neuroblastoma: a case report. J Indian Assoc Pediatr Surg. 2002;7:76–9.
35. Khandakar B, Maiti M, Dey S, Sen P, Bhattacharya P, Sarkar R. Primary pediatric renal primitive neuroectodermal tumour: a case report and review of literature. Turk Pathol. 2018;34:251–4. https://doi.org/10.5146/tjpath.2015.01340.
36. Celli R, Cai G. Ewings sarcoma/primitive neuroectodermal tumour of kidney: a rare and lethal entity. Arch Pathol Lab Med. 2016;140:281–5. https://doi.org/10.5858/arpa.2014-0367-RS.

37. Zollner S, Dorksen U, Jurgen H, Ranft A. Renal Ewing tumour. Ann Oncol. 2013;24:2455–61. https://doi.org/10.1093/annonc/mdt215.
38. Dobkin S, Brem AS, Caldmone AA. Primary renal lymphoma. J Urol. 1991;146:1588–90. https://doi.org/10.1016/s0022-5347(17)38174-0.
39. Dhull VS, Mukherjee A, Karunanithi S, Durgapal P, Bal C, Kumar R. Bilateral primary renal lymphoma in a pediatric patient: staging and response to treatment with F^{18}-FDG PET/CT. Rev Esp Med Nucl Imagen Mol. 2015;34:49–52. https://doi.org/10.1016/j.remn.2014.05.004.
40. William SM, Killen AA. Tumour lysis syndrome. Arch Pathol Lab Med. 2019;143:386–93. https://doi.org/10.5858/arpa.2017-0278-RS.
41. Flum AS, Hamoui N, Said MA, Yang XJ, Casalino DD, McGuire BB, et al. Update on the diagnosis and management of renal angiomyolipoma. J Urol. 2016;195:834–46. https://doi.org/10.1016/j.juro.2015.07.126.
42. Lienert AR, Nicol D. Renal angiomyolipoma. BJU Int. 2012;110(Suppl 4):25–7. https://doi.org/10.1111/j.1464-410X.2012.11618.x.
43. Tchaprassian Z, Mognato G, Paradias G, D'Amore ES, Tregnaghi A, Cecchetto G. Renal angiomyolipoma in children: diagnostic difficulty in 3 patients. J Urol. 1998;159:1654–6. https://doi.org/10.1097/00005392-199805000-00083.
44. Springer AM, Saxena AK, Willital GH. Angiomyolipoma with hypertension mimicking a malignant renal tumor. Pediatr Surg Int. 2002;18:526–8. https://doi.org/10.1007/s00383-002-0774-7.
45. Razik A, Das CJ, Sharma S. Angiomyolipoma of the kidneys: current perspectives and challenges in diagnostic imaging and image-guided therapy. Curr Probl Diagn Radiol. 2019;48:251–61. https://doi.org/10.1067/j.cpradiol.2018.03.006.
46. Sarin YK, Sengar M. Cystic nephroma. Indian Pediatr. 2005;42:84–6.
47. Vujanić GM, Jenney MEM, Adams H, Meyrick SM. Juxtaposed cystic nephroma and Wilms' tumor. Pediatr Dev Pathol. 2000;3:91–4. https://doi.org/10.1007/s100240050012.
48. Dowerah S, Borgohain M. Cystic partially differentiated nephroblastoma: a rare case report. Ann Path Lab Med. 2015;2:C155–8.
49. Kurian JJ, Jehangir S, Korula A. Multiloculated cystic renal tumors of childhood: has the final word been spoken. J Indian Assoc Pediatr Surg. 2018;23:22–6. https://doi.org/10.4103/jiaps.JIAPS_224_16.
50. Babut JM, Bawab F, Jouan H, Coeurdacier P, Treguier C, Fremond B. Renal cystic tumours in children—a diagnostic challenge. Eur J Pediatr Surg. 1993;3:157–60. https://doi.org/10.1055/s-2008-1063533.
51. van den Hoek J, de Krijger R, van de Ven K, Lequin M, van den Heuvel-Eibrink MM. Cystic nephroma, cystic partially differentiated nephroblastoma and cystic Wilms' tumor in children: a spectrum with therapeutic dilemmas. Urol Int. 2009;82:65–70. https://doi.org/10.1159/000176028.
52. Raj P, Khanolkar A, Sarin YK. Metanephric adenofibroma masquerading as Wilms tumour. APSP J Case Rep. 2016;7:37. https://doi.org/10.21699/ajcr.v7i5.463.